Eur. Phys. J. D (2014) 68: 340
DOI: 10.1140/epjd/e2014-50381-2

THE EUROPEAN PHYSICAL JOURNAL D

Regular Article

Theoretical study on the interaction of electron-acoustic shock waves in a generalized Lorentzian plasma

Jiu-Ning Han[1,a], Jun-Xiu Li[2], Jian-Xiong Gu[1], Zhen-Hai Han[1], and Ya-Gong Nan[1]

[1] College of Physics and Electromechanical Engineering, Hexi University, Zhangye 734000, P.R. China
[2] College of Civil Engineering, Hexi University, Zhangye 734000, P.R. China

Received 14 May 2014 / Received in final form 4 August 2014
Published online 6 November 2014 –

Abstract. The nonlinear interaction between electron-acoustic shock waves in a dissipative, non-Maxwellian plasma composed of cold fluid electrons, stationary background ions, and inertialess superthermal electrons has been studied. The effects of plasma parameters on the trajectory changes (i.e., phase shifts) of shock waves after their head-on collision is our main concern. The results indicate that the interactions between shocks are different from those of solitons. Also, it is found that the occurrence and variation of trajectory shifts may be due to the combined role played by the dispersion and dissipation of the colliding nonlinear structure.

1 Introduction

Electron-acoustic wave (EAW) is electrostatic plasma wave with an unusually small phase velocity compared to Langmuir wave. The name of this wave mode suggests that electrons are involved in the wave dynamics, and therefore, it is a high frequency wave. This wave can exist in an unmagnetized plasma with three components, namely, highly dense energetic electrons which we often call as hot electrons, diluted cold electrons, and massive ions. These two electron components are obviously different from each other, because the hot electron component has energy of the order of KeV, while the cold electron component has energy not greater than 60 eV [1]. Ions have less energy in comparison with electrons, therefore, this component is not taking part in the EAW dynamics, they just serve as a stationary charge neutral back ground. What happens physically is that the mass of the cold electrons provides the inertia, while the restoring force comes from the pressure of the inertialess hot electrons.

EAW is similar to the ion-acoustic wave (IAW), the difference is that for this wave mode, the cold electrons do the same job as the ions do in the usual IAW. In contrast to the IAW, EAW usually suffers strong damping, this is because the cold electrons have the easier mobility than ions. The propagation of EAW is only possible within a restricted range of the plasma parameter values, since Landau damping will become stronger when the wave phase velocity approaches the thermal velocity of cold (hot) electron component. EAWs were found in many spacecraft observations and experimental studies. For example, the observations by the FAST in the intermediate auroral region (altitude <4000 km) [2], as well as the observations by the POLAR at higher altitude auroral region (between $2R_E \sim 8R_E$, R_E being earth's radius) [3], these finding confirm the existence of EAWs in several parts of magnetosphere [4–6]. Experimentally, in reference [7], Montgomery et al. have pointed out that EAW can also be excited in laboratory plasma with two electron components. Motivated by these observations, a number of efforts on modelling methods have been made to understand the properties of EAWs in such plasma systems. Recently, Kourakis and Shukla [8] presented a theoretical and numerical study on the amplitude modulation of EAWs propagating in space plasmas whose constituents are inertial cold electrons, Boltzmann distributed hot electrons, and stationary ions, it is shown that their system can exist different types of localized EAW excitations. More recently, Baluku et al. [9] studied the EAW in a plasma kinetic model which treats both the cool and the hot electrons as having a kappa velocity distribution. Using a particle-in-cell simulation, Koen et al. [10] discussed the characteristics of electron plasma and EAWs in plasmas containing an ion and two electron components. The electron velocities are modeled by a combination of two κ distributions.

In the natural space environment, e.g., planetary magnetospheres, astrophysical plasmas, and the solar wind, plasmas are generally observed to possess a non-Maxwellian high-energy tai1 [11–13]. Superthermal particles may arise due to the effect of external force acting on the natural space environment plasmas or to wave-particle

[a] e-mail: hanjiuning@126.com

interactions. A useful distribution function to model such plasmas is the generalized Lorentzian (kappa) distribution. It is shown that kappa distribution rather than Maxwellian distribution gives a better fit to the observed physical phenomena. For vary larger values of the spectral index κ (i.e., $\kappa \to \infty$), the kappa distribution reduces to the Maxwellian distribution, while for smaller values of κ, it represents a strong high-energy tail having a power-law form distribution function. During the past several years, a great deal of interest has been shown on the properties of linear and nonlinear wave modes with superthermal particles in various plasma systems (see for examples, Refs. [14–16]).

It is generally known that wave-wave interaction is one of important physical phenomena in nonlinear physics, during the last several years, there has been a growing interest in the investigation of head-on collision between solitons in various plasma models, the basic features of this nonlinear phenomenon are well understood now. In a recent paper, Harvey et al. [17] experimentally and numerically studied the interaction of two counter propagating solitons of equal amplitudes in a monolayer strongly coupled complex plasma, their finding confirm the knowledge of previous studies about soliton interactions. More recently, Verheest et al. [18] investigated the head-on collision of electrostatic solitons in a plasma composed of a number of cold (positive and negative) ion species and Boltzmann electrons. Eslami et al. [19] discussed the head-on collision of EAWs in unmagnetized plasma with nonextensive plasma hot electrons. Theoretical and experimental papers in the literature shown that there are positive or negative phase shifts after the soliton interactions. However, up to now, to the best of our knowledge, there are rare investigations consider the problem of interaction between shock waves. Therefore, the aim of the present study is to study the head-on collision between two electron-acoustic shock waves (EASWs) in a generalized Lorentzian plasma with κ distributed superthermal electrons. The effects of plasma parameters, especially the superthermal effect on the trajectory shifts of shock waves after their interaction will be our may concern.

The paper is organized as follows. In the second section, the basic set of fluid equations for the electrostatic wave are presented. In the third section, we derive two Korteweg-de Vries-Burgers (KdV-Burgers) equations governing the nonlinear dynamics of the EASWs. In the fourth section, the numerical results and discussion are given, while the last section is kept for conclusion.

2 Basic set of equations

In order to construct the model, we consider a unbounded, homogeneous, collisionless, and unmagnetized plasma system consisting of three components, namely cold fluid electrons, inertialess hot electrons with a generalized Lorentzian (κ) velocity distribution, and uniformly distributed stationary ions. Now the governing equations of the cold electron fluid are given by the following set of equations.

$$\frac{\partial N_c}{\partial t} + \frac{\partial (N_c U_c)}{\partial x} = 0, \tag{1}$$

$$\frac{\partial U_c}{\partial t} + U_c \frac{\partial U_c}{\partial x} + \frac{\sigma}{N_c}\frac{\partial P_c}{\partial x} = \frac{\partial \Psi}{\partial x} + \eta_e \frac{\partial^2 U_c}{\partial x^2}, \tag{2}$$

$$\frac{\partial P_c}{\partial t} + U_c \frac{\partial P_c}{\partial x} + \gamma P_c \frac{\partial U_c}{\partial x} = 0, \tag{3}$$

$$\frac{\partial^2 \Psi}{\partial x^2} = N_c + \beta N_h - \beta - 1. \tag{4}$$

In the above equations, N_c and N_h are the cold and hot electron number densities, respectively. $\sigma = T_c/T_h$, ε_0 is the permittivity constant and e is the magnitude of the elementary charge. Here, the electrostatic wave potential Ψ is normalized by $k_B T_h/e$, the cold electron fluid velocity U_c and pressure P_c are respectively normalized by the EA speed $c_e = (k_B T_h/m_e)^{1/2}$ and $N_{c0} k_B T_c$. The space coordinate x and time coordinate t are normalized by the electron Debye length $\lambda_D = \sqrt{\varepsilon_0 k_B T_h/N_{c0} e^2}$ and the electron plasma period $\omega_{pc}^{-1} = \sqrt{\varepsilon_0 m_e/N_{c0} e^2}$, respectively. In addition, at equilibrium, we have $Z N_{i0} = N_{c0} + N_{h0}$, where N_{i0}, N_{c0}, and N_{h0} are the unperturbed ion, cold and hot electron number densities, respectively. It is shown that $Z N_{i0}/N_{c0} = 1 + \beta$, in which $\beta = N_{h0}/N_{c0}$ is the unperturbed hot-to-cold electron number density ratio. According to the results given in references [20,21], Landau damping is minimized in the situation of $0.25 \leq \beta \leq 4$. η_e is the coefficient of electron kinematic viscosity, it arises by considering the kinematic viscosity among the plasma constituents. $\gamma = (d+2)/d$ indicates the specific heat ratio, where d denotes the freedom degree of the system. In the present study, we shall use $\gamma = 3$ (viz., $d = 1$) for the adiabatic cold electrons.

To model the hot electron distribution, we employ a three-dimensional generalized Lorentzian(or κ) distribution function, which takes the following form [22,23]:

$$f_\kappa(v_h) = \frac{N_{h0}}{(\pi\kappa\theta^2)^{3/2}} \frac{\Gamma(\kappa+1)}{\Gamma(\kappa-\frac{1}{2})} \left(1 + \frac{v_h^2}{\kappa\theta^2}\right)^{-\kappa-1}, \tag{5}$$

where $\theta^2 = [(\kappa - 3/2)/\kappa](2k_B T_h/m)$, θ is the effective thermal speed, modified by spectral index κ. N_{h0} is the equilibrium number density of the hot electrons, and T_h is the kinetic temperature. $\Gamma(x)$ is the gamma function which arises from the normalization of $f_\kappa(v_h)$. It should be noted that for a physically realistic thermal speed, one requires $\kappa > 3/2$.

Integrating the kappa distribution over the velocity space, the hot electron number density are given as

$$N_h = N_{h0}\left[1 - \frac{e\Psi}{(\kappa - \frac{3}{2})k_B T_h}\right]^{-\kappa+\frac{1}{2}}. \tag{6}$$

And then, it can be written in dimensionless form as

$$N_h = \left(1 - \frac{\Psi}{\kappa - \frac{3}{2}}\right)^{-\kappa+\frac{1}{2}}. \tag{7}$$

3 Derivation of KdV-Burgers equation

To investigate the head-on collision between two shock waves propagating in opposite directions along x-axis, we assume that, there are two shock waves in the plasma, they are, asymptotically, far apart in the initial state and travel toward each other. After some time, they meet, collide, and then separate away. We also assume that the interaction between two shocks are weak, ideally, we expect that the collision will be quasi-elastic. The extended Poincaré-Lighthill-Kuo perturbation method is a useful method to investigate the effects of collision on the propagation of nonlinear waves. By using this method, a number of studies have been made to discuss the head-on collisions of planar or nonplanar solitary waves in various kinds of plasma systems [24–27]. It is generally known that in a plasma system, the presence of electron kinematic viscosity can introduce a dissipation that causes the Burgers term and this is responsible for the generation of EASW. The formation of these shocks is due to the balance between the nonlinearity and the combined effect of dispersion and dissipation, their dynamics are governed by the usual KdV-Burgers equation. In a dissipation plasma system, several papers in the literature confirm the existence of both monotonic and oscillatory dispersive shock waves. Considering the dissipative mechanism of KdV-Burgers equation, in order to study the head-on collision between two shock waves, we use the stationary propagation shock solution in the present study. To model the head-on colliding process of two shock waves, first, we introduce the following co-ordinates transformations (wave frames):

$$\xi = \epsilon(x - \lambda t) + \epsilon^2 M^{(0)}(\eta, \tau) + \ldots, \tag{8}$$

$$\eta = \epsilon(x + \lambda t) + \epsilon^2 N^{(0)}(\xi, \tau) + \ldots, \tag{9}$$

$$\tau = \epsilon^3 t, \tag{10}$$

where ϵ is a smallness formal perturbation parameter, which characterizes the strength of nonlinearity. Subsequently, for convenience, we denote the right-going and left-going waves by superscripts R and L, and ξ and η denote the trajectories of the two shock waves R and L, respectively. Next, we expand quantities N_c, U_c, P_c and Ψ about their equilibrium values in power series of ϵ

$$\Pi = \Pi^{(0)} + \sum_{n=1}^{\infty} \epsilon^{(n+1)} \Pi^{(n)}, \tag{11}$$

where

$$\Pi = \left[N_c \; U_c \; P_c \; \Psi \right]^T,$$

$$\Pi^{(n)} = \left[N_c^{(n)} \; U_c^{(n)} \; P_c^{(n)} \; \Psi^{(n)} \right]^T,$$

and

$$\Pi^{(0)} = [1 \; 0 \; 1 \; 0]^T.$$

Considering the value of electron kinematic viscosity η_e is small in many experimental situations, so we set its value as $\eta_e = \epsilon\eta_0$. Then, substituting equations (8)–(11) into equations (1)–(4), we obtain a set of coupled equations in different orders of ϵ. To the leading order, we have

$$\lambda \left(\frac{\partial N_c^{(1)}}{\partial \eta} - \frac{\partial N_c^{(1)}}{\partial \xi} \right) + \left(\frac{\partial U_c^{(1)}}{\partial \xi} + \frac{\partial U_c^{(1)}}{\partial \eta} \right) = 0, \tag{12}$$

$$\lambda \left(\frac{\partial U_c^{(1)}}{\partial \eta} - \frac{\partial U_c^{(1)}}{\partial \xi} \right) + \sigma \left(\frac{\partial P_c^{(1)}}{\partial \xi} + \frac{\partial P_c^{(1)}}{\partial \eta} \right) = \frac{\partial \Psi^{(1)}}{\partial \xi} + \frac{\partial \Psi^{(1)}}{\partial \eta}, \tag{13}$$

$$\lambda \left(\frac{\partial P_c^{(1)}}{\partial \eta} - \frac{\partial P_c^{(1)}}{\partial \xi} \right) + 3 \left(\frac{\partial U_c^{(1)}}{\partial \xi} + \frac{\partial U_c^{(1)}}{\partial \eta} \right) = 0, \tag{14}$$

$$N_c^{(1)} = -\chi \Psi^{(1)}, \tag{15}$$

where $\chi = \beta^{\frac{\kappa - \frac{1}{2}}{\kappa - \frac{3}{2}}}$, from equations (12)–(15), one can get the following relations

$$N_{cR}^{(1)}(\xi, \tau) = -\chi \Psi_R^{(1)}(\xi, \tau), \tag{16}$$

$$N_{cL}^{(1)}(\eta, \tau) = -\chi \Psi_L^{(1)}(\eta, \tau), \tag{17}$$

$$U_{cR}^{(1)}(\xi, \tau) = -\lambda\chi \Psi_R^{(1)}(\xi, \tau), \tag{18}$$

$$U_{cL}^{(1)}(\eta, \tau) = \lambda\chi \Psi_L^{(1)}(\eta, \tau), \tag{19}$$

$$P_{cR}^{(1)}(\xi, \tau) = -3\chi \Psi_R^{(1)}(\xi, \tau), \tag{20}$$

$$P_{cL}^{(1)}(\eta, \tau) = -3\chi \Psi_L^{(1)}(\eta, \tau). \tag{21}$$

As mentioned before, $\Psi_R^{(1)}(\xi, \tau)$ and $\Psi_L^{(1)}(\eta, \tau)$ describe the right-going and left-going shock waves, which propagate in opposite directions along the trajectories ξ and η, respectively. The wave velocity λ also can be obtained as $\lambda^2 = 3\sigma + \frac{1}{\chi}$.

To the next higher order of ϵ, we obtain a set of equations as follows:

$$\frac{\partial \Psi_R^{(1)}}{\partial \tau} + P\Psi_R^{(1)} \frac{\partial \Psi_R^{(1)}}{\partial \xi} + Q \frac{\partial^3 \Psi_R^{(1)}}{\partial \xi^3} - R_1 \frac{\partial^2 \Psi_R^{(1)}}{\partial \xi^2} = 0, \tag{22}$$

$$\frac{\partial \Psi_L^{(1)}}{\partial \tau} + P\Psi_L^{(1)} \frac{\partial \Psi_L^{(1)}}{\partial \eta} + Q \frac{\partial^3 \Psi_L^{(1)}}{\partial \eta^3} - R_2 \frac{\partial^2 \Psi_L^{(1)}}{\partial \eta^2} = 0, \tag{23}$$

and

$$2\frac{\partial M^{(0)}}{\partial \eta} = \Gamma \Psi_L^{(1)}, \tag{24}$$

$$2\frac{\partial N^{(0)}}{\partial \xi} = \Gamma \Psi_R^{(1)}, \tag{25}$$

where

$$P = -\frac{\varpi + 3\chi^2 + 12\sigma\chi^3}{2\lambda^2\chi^2}, \quad Q = \frac{1}{2\lambda^2\chi^2}, \quad R_1 = \frac{\eta_0}{2\lambda},$$

$$R_2 = -\frac{\eta_0}{2\lambda}, \quad \Gamma = \frac{\varpi - \chi^2}{2\lambda^2\chi^2}, \quad \text{and} \quad \varpi = \frac{\chi(\kappa + \frac{1}{2})}{\kappa - \frac{3}{2}}.$$

Table 1. Location of the colliding shock waves $\Psi_R^{(1)}$ and $\Psi_L^{(1)}$ in terms of asymptotic values of ξ and η.

	Before collision	After collision
Right-going $\Psi_R^{(1)}$	$\eta \to -\infty$	$\eta \to +\infty$
Left-going $\Psi_L^{(1)}$	$\xi \to +\infty$	$\xi \to -\infty$

It is clear that equations (22) and (23) are the two-side traveling wave KdV-Burgers equations in the reference frames of ξ and η. The dissipative terms in the right-hand side of equations (22) and (23) represent the Burgers term, arising due to the kinematic viscosity among the plasma constituents. It is obviously shown that the nonlinear coefficient P is negative, it implies the existence of a kink-type shock shape. According to the discussion of the paper by Kourakis et al. [28], the corresponding stationary propagation shock wave solutions of EASWs governed by equations (22) and (23) take the following form:

$$\Psi_R^{(1)} = \frac{3R_1^2}{25PQ}\left[1 - \tanh^2 \Xi_1 + 2(1 - \tanh \Xi_1)\right], \quad (26)$$

$$\Psi_L^{(1)} = \frac{3R_2^2}{25PQ}\left[1 - \tanh^2 \Xi_2 + 2(1 - \tanh \Xi_2)\right], \quad (27)$$

where

$$\Xi_1 = \frac{R_1}{10Q}(\xi - \frac{6R_1^2}{25Q}\tau - X_0), \quad \Xi_2 = \frac{R_2}{10Q}(\eta - \frac{6R_2^2}{25Q}\tau - Y_0).$$

X_0 and Y_0 are two real constants, they represent the initial wave positions of shock waves R and L, respectively, τ is the stretched time coordinate representing the slow time scale.

We now identify the right- and left-going waves as $\psi_R^{(1)}$ and $\psi_L^{(1)}$, respectively. The location of these waves before and after collision in terms of asymptotic values of ξ and η are specified in Table 1. And then, the phase functions $M^{(0)}$ and $N^{(0)}$ can be calculated as

$$M^{(0)} = \frac{\Gamma}{2}\int_{-\infty}^{\eta} \Psi_L^{(1)}(\eta, \tau)d\eta$$

$$= \frac{\Gamma}{10P}(\Theta_B|_{\eta=\eta} - \Theta_B|_{\eta=-\infty}), \quad (28)$$

$$N^{(0)} = \frac{\Gamma}{2}\int_{+\infty}^{\xi} \Psi_R^{(1)}(\xi, \tau)d\xi$$

$$= \frac{\Gamma}{10P}(\Theta_A|_{\xi=\xi} - \Theta_A|_{\xi=+\infty}), \quad (29)$$

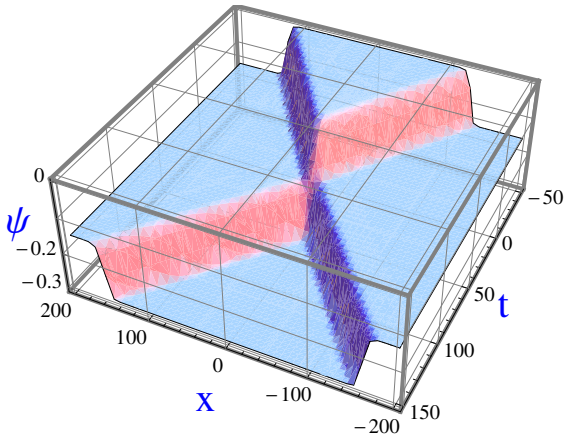

Fig. 1. Profile of head-on collision process between two same structures EA shock waves, the parameters are given as: $\kappa = 2$, $\beta = 1$, $\sigma = 0.01$, $\eta_0 = 0.7$, $X_0 = -30$, and $Y_0 = 30$.

where,

$$\Theta_A = \frac{6R_1^2\xi}{5Q} - 12R_1 \log \Upsilon_A + 6R_1\Lambda_A,$$

$$\Theta_B = \frac{6R_2^2\eta}{5Q} - 12R_2 \log \Upsilon_B + 6R_2\Lambda_B,$$

$$\Upsilon_A = \cosh\left[\frac{R_1\xi}{10Q} - \frac{R_1}{250Q^2}\left(6R_1^2\tau + 25Q\xi\right)\right],$$

$$\Upsilon_B = \cosh\left[\frac{R_2\eta}{10Q} - \frac{R_2}{250Q^2}\left(6R_2^2\tau + 25Q\eta\right)\right],$$

$$\Lambda_A = \tanh\left\{\frac{R_1}{250Q^2}\left[-6R_1^2\tau + 25Q(\xi - X_0)\right]\right\},$$

$$\Lambda_B = \tanh\left\{\frac{R_2}{250Q^2}\left[-6R_2^2\tau + 25Q(\eta - Y_0)\right]\right\}.$$

4 Results and discussions

To examine the effect of collision on the propagation of shock waves, in this section, we numerically study the results obtained in the above section. As shown in Figure 1, the red and blue shocks respectively represent the right-going wave $\Psi_R^{(1)}$ and left-going wave $\Psi_L^{(1)}$. Those two colliding shocks are described by equations (26) and (27) and propagate along the ξ and η trajectories, respectively. It is clear that the interactions between shock waves are different from those between solitary waves. For soliton interaction, the results suggest that during the wave collision process, one practically motionless composite nonlinear structure will be generated, this structure survives during some time interval, the amplitude of the structure is larger than those colliding solitary waves and the velocity of the structure depends on the colliding wave heights. However, for shock interaction, clearly, there is no new structure formed in their colliding region, the interaction will only induce a change of propagation trajectories.

Figures 2–5 show the effects of the superthermal parameter κ, the electron temperature ratio σ, the electron

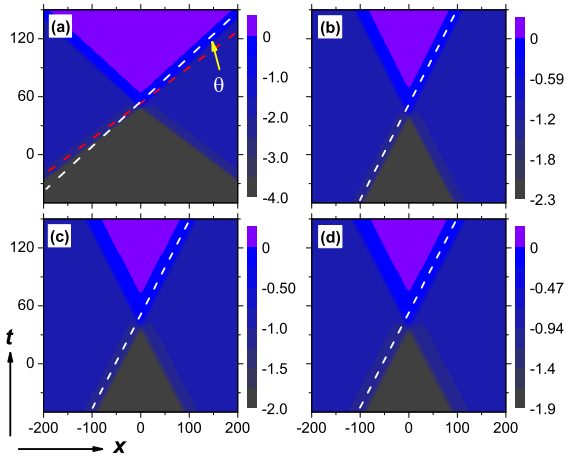

Fig. 2. Showing the effect of superthermal parameter κ on the colliding process of shock waves ($\times 10^{-1}$) for various values of (a) $\kappa = 2$; (b) $\kappa = 3$; (c) $\kappa = 4$; (d) $\kappa = 5$. Other parameters are set as: $\beta = 1$, $\sigma = 0.01$, $\eta_0 = 0.8$, $X_0 = -30$, and $Y_0 = 30$.

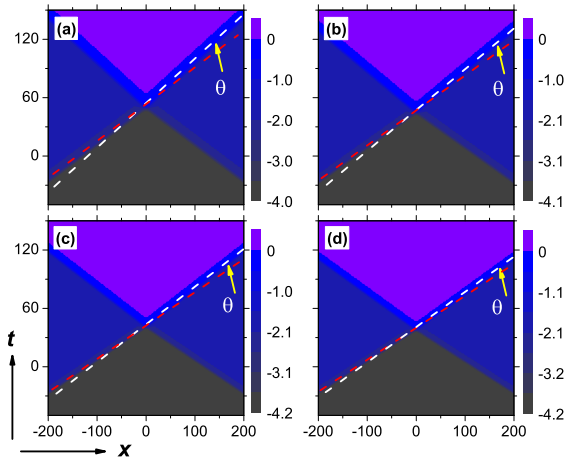

Fig. 3. Showing the effect of electron temperature ratio σ on the colliding process of shock waves ($\times 10^{-1}$) for various values of (a) $\sigma = 0.01$; (b) $\sigma = 0.04$; (c) $\sigma = 0.07$; (d) $\sigma = 0.10$. Other parameters are set as: $\kappa = 2$, $\beta = 1$, $\eta_0 = 0.8$, $X_0 = -30$, and $Y_0 = 30$.

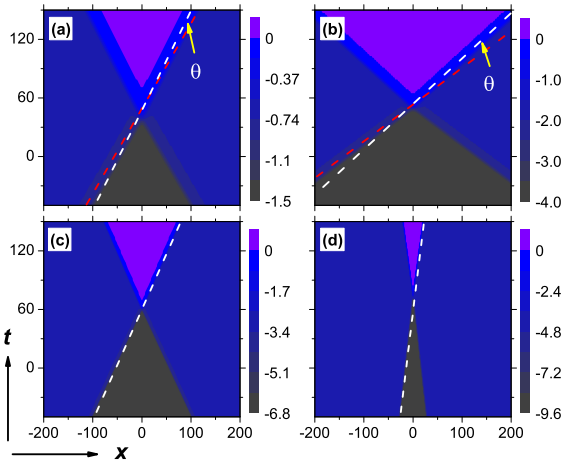

Fig. 4. Showing the effect of electron number density ratio β on the colliding process of shock waves ($\times 10^{-1}$) for various values of (a) $\beta = 0.5$; (b) $\beta = 1.0$; (c) $\beta = 1.5$; (d) $\beta = 2$. Other parameters are set as: $\kappa = 2$, $\sigma = 0.01$, $\eta_0 = 0.8$, $X_0 = -30$, and $Y_0 = 30$.

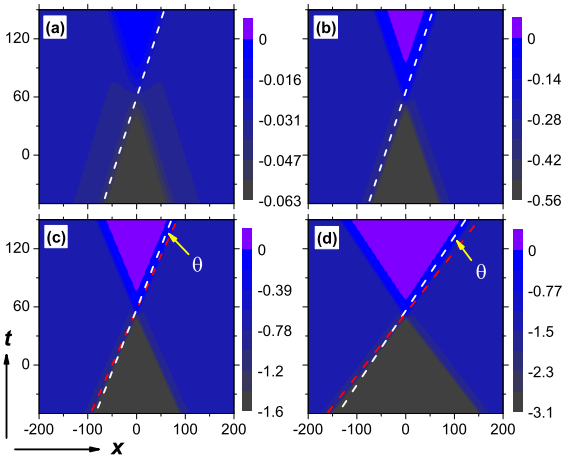

Fig. 5. Showing the effect of electron kinematic viscosity η_0 on the colliding process of shock waves ($\times 10^{-1}$) for various values of (a) $\eta_0 = 0.1$; (b) $\eta_0 = 0.3$; (c) $\eta_0 = 0.5$; (d) $\eta_0 = 0.7$. Other parameters are set as: $\kappa = 2$, $\sigma = 0.01$, $\beta = 1$, $X_0 = -30$, and $Y_0 = 30$.

number density ratio β, and the normalized electron kinematic viscosity η_0 on the trajectory changes (phase shifts) of the colliding shock waves, respectively. As shown in these figures, the brightness corresponding to the relative wave amplitude value, the red dashed lines marked the shock wave paths when the waves propagate alone, and the white dashed lines marked the shock wave paths after their head-on collision. As the yellow arrows pointed out, before and after the interaction, there is a angle between the wave paths for each colliding shocks. This is obviously different from the results obtained for soliton interactions. It is generally known that the head-on collision of solitary wave can induce positive or negative trajectory changes (phase shifts). That is to say, the colliding waves quicken or slower their velocities after the interaction. Furthermore, whether the phase shifts are positive or negative, the trajectories before and after wave interaction are parallel (see Refs. [17,29]). However, for shock interaction, the wave paths before and after collision are not parallel. That is, for the colliding shocks, there are shifts of the propagation trajectory after their collisions, more importantly, the propagation directions of the colliding shocks are changed.

The results obtained in Figures 2–5 are shown in Table 2, here, let us introduce a new parameter θ, here θ refer to the angle between the wave path for each colliding shock wave before and after the interaction, i.e., the shift of propagation trajectory. First of all, let us examine the effect of the electron kinematic viscosity η_0 on the interaction of shock waves. It is found that the trajectory changes increase with the increase of η_0. To explain the above phenomenon, we need to make a detailed analysis

Table 2. Effects of the plasma parameters κ, σ, β, and η_0 on the trajectory changes θ (in °) of the colliding EA shock waves.

κ	Angle	σ	Angle	β	Angle	η_0	Angle
2	$\theta = 9$	0.01	$\theta = 9$	0.5	$\theta = 6$	0.1	$\theta = 0$
3	$\theta = 0$	0.04	$\theta = 8$	1.0	$\theta = 9$	0.3	$\theta = 0$
4	$\theta = 0$	0.07	$\theta = 7$	1.5	$\theta = 0$	0.5	$\theta = 5$
5	$\theta = 0$	0.10	$\theta = 6$	2.0	$\theta = 0$	0.7	$\theta = 8$

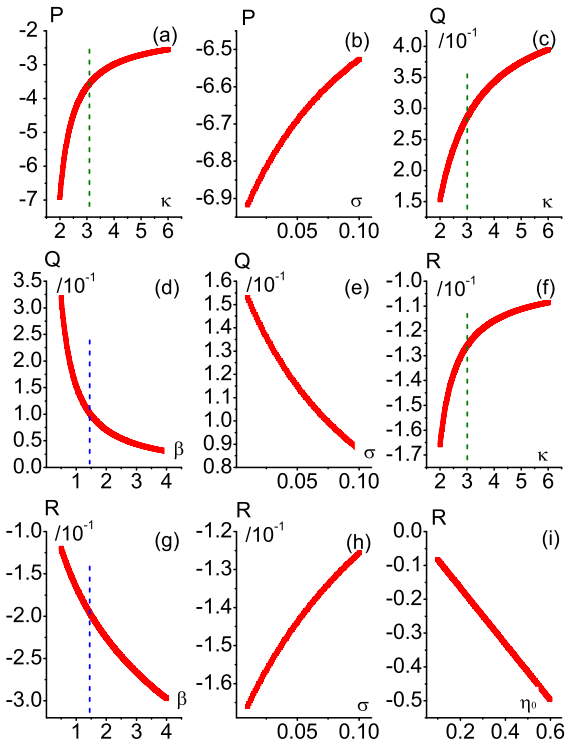

Fig. 6. Effects of plasma parameters on the nonlinearity, dispersion, and dissipation coefficients of colliding shock waves.

of the effects of plasma parameters on the nonlinearity, dispersion and dissipation coefficients of colliding shocks. Combined with the results shown in Figure 6, we may say that dissipation has a decisive effect on the occurrence of trajectory shift, and the increase in the dissipation leads to an increase in the trajectory shift. Furthermore, the trajectory shifts will appear only when the dissipation of the system (i.e., the value of η_0) is large enough.

Secondly, let's consider the electron number density ratio β. It is shown that angle θ increases with the increase of β for smaller values of density ratio. However, with the increase of β, one can clearly note that there are no trajectory changes for bigger values of β (i.e., $\beta = 1.5$ and 2.0). For the physical mechanism of this phenomenon, it may be due to the combined role played by the dispersion and dissipation of the nonlinear structure. First, let us take a look at Figure 6g, it is shown that dissipative coefficient $|R|$ increases with the increase of β, this is the mainly reason for the increase of θ at the beginning. In addition, the changing of the curve is relatively uniform, therefore, the variation of dissipation can not lead the disappearance of trajectory change later; second, from Figure 6d, we note that dispersive coefficient Q decreases sharply with the increase of β at the range of 0.5 to 1.5, and then the decreasing rate become slowly at the range of 1.5 to 2.0, the slowly decreasing rate just leads to the disappearance of the trajectory shifts. Thus, we can predictably conclude that there are two roles that maybe account for this phenomenon, the increasing role played by the dissipation, and the decreasing role played by the dispersion. Obviously, when the decreased effect is larger than the increased effect, there are no trajectory shifts for the colliding shock.

Thirdly, for electron temperature ratio σ, it is clear that θ uniformly decreases with the increase of σ, this changing trend is the same as the trends of the nonlinearity, the dissipative, and the dissipative coefficients change with σ (see Figs. 6b, 6e, and 6h, respectively). And lastly, let us investigate the superthermal parameter κ on the trajectory changes. It is found that except for the strong superthermal case (small spectral index $\kappa = 2$), for the cases of $\kappa = 3, 4, 5$, there are no shifts of wave trajectories. To get a better understanding of this phenomenon, we take the value of $\kappa = 1.7$ as an academic study, and we get a result of $\theta = 10°$, this makes us to think that the trajectory change decreases with the increase of κ. Combined with the results shown in Figure 6, we may say that there are two contributions that maybe account for these phenomena, first, the decreasing role played by the dissipation, it decreases with the increase of κ, and when the dissipation of the system is small enough, we already know that there is no trajectory shift for the colliding shock; second, the decreasing role played by the dispersion, it is clear that dispersive coefficient increases with κ, this effectively leads to the disappearance of trajectory shifts.

5 Conclusion

Summarizing our results, we have studied the head-on collision of shock waves in a three-component plasma composed of cold fluid electrons, uniformly distributed stationary ions, and inertialess κ distributed hot electrons. It is shown that the interactions between shock waves are obviously different from those between solitary waves. First, there is no newly formed nonlinear structure during the colliding process of shocks; second, the head-on collision can induce the shifts of wave propagation direction, that is, the trajectories of colliding shocks before and after interaction are not parallel, there is a angle between those two paths. Also, it is found that dissipation has a decisive effect on the occurrence of trajectory changes, and the variation of trajectory shifts may be due to the combined role played by the dispersion and dissipation of the colliding nonlinear structure. Furthermore, when the decreasing role made by dispersion is larger than the increasing role made by dissipation, or the combined effect of these two roles reach a balanced state, there will be no trajectory changes in the present system.

The authors acknowledge the financial support from the National Natural Science Foundation of People's Republic of China under Grant No. 11365007.

References

1. M. Dutta, N. Chakrabarti, R. Roychoudhury, M. Khan, Phys. Plasmas **18**, 102301 (2011)
2. R.E. Ergun, C.W. Carlson, J.P. McFadden, F.S. Mozer, G.T. Delory, W. Peria, C.C. Chaston, M. Temerin, I. Roth, L. Muschietti, R. Elphic, R. Strangeway, R. Pfaff, C.A. Cattell, D. Klumpar, E. Shelley, W. Peterson, E. Moebius, L. Kistler, Geophys. Res. Lett. **25**, 2041 (1998)
3. J.R. Franz, P.M. Kintner, J.S. Pickett, Geophys. Res. Lett. **25**, 1277 (1998)
4. H. Matsumoto, H. Kojima, T. Miyatake, Y. Omura, M. Okada, I. Nagano, M. Tsutsui, Geophys. Res. Lett. **21**, 2915 (1994)
5. C.A. Cattell, J. Dombeck, J.R. Wygant, M.K. Hudson, F.S. Mozer, M.A. Temerin, W.K. Peterson, C.A. Kletzing, C.T. Russell, R.F. Pfaff, Geophys. Res. Lett. **26**, 425 (1999)
6. B. Tsurutani, J.K. Arballo, G.S. Lakhina, C.M. Ho, B. Buti, J.S. Pickett, D.A. Gurnett, Geophys. Res. Lett. **25**, 4117 (1998)
7. D. Montgomery, R.J. Focia, H.A. Rose, D.A. Russell, J.A. Cobble, J.C. Fernandez, R.P. Johnson, Phys. Rev. Lett. **87**, 155001 (2001)
8. I. Kourakis, P.K. Shukla, Phys. Rev. E **69**, 036411 (2004)
9. T.K. Baluku, M.A. Hellberg, R.L. Mace, J. Geophys. Res. **116**, A04227 (2011)
10. E.J. Koen, A.B. Collier, S.K. Maharaj, Phys. Plasmas **19**, 042102 (2012)
11. T.Y. Lui, S.M. Krimigis, Geophys. Res. Lett. **8**, 527 (1981)
12. A.T.Y. Lui, S.M. Krimigis, Geophys. Res. Lett. **10**, 13 (1983)
13. D.J. Williams, D.G. Mitchell, S.P. Christon, Geophys. Res. Lett. **15**, 303 (1988)
14. B. Sahu, Europhys. Lett. **101**, 55002 (2013)
15. A. Danehkar, N.S. Saini, M.A. Hellberg, I. Kourakis, Phys. Plasmas **18**, 072902 (2011)
16. J.N. Han, W.S. Duan, J.X. Li, Y.L. He, J.H. Luo, Y.G. Nan, Z.H. Han, G.X. Dong, Phys. Plasmas **21**, 012102 (2014)
17. P. Harvey, C. Durniak, D. Samsonov, G. Morfill, Phys. Rev. E **81**, 057401 (2010)
18. F. Verheest, M.A. Hellberg, W.A. Hereman, Phys. Plasmas **19**, 092302 (2012)
19. P. Eslami, M. Mottaghizadeh, H.R. Pakzad, Astrophys. Space Sci. **338**, 271 (2012)
20. S.P. Gary, R.L. Tokar, Phys. Fluids **28**, 2439 (1985)
21. R.L. Tokar, S.P. Gary, Geophys. Res. Lett. **11**, 1180 (1984)
22. D. Summers, R.M. Thorne, Phys. Fluids B **3**, 1835 (1991)
23. M.A. Hellberg, R.L. Mace, T.K. Baluku, I. Kourakis, N.S. Saini, Phys. Plasmas **16**, 094701 (2009)
24. J.K. Xue, Phys. Rev. E **69**, 016403 (2004)
25. F. Verheest, M.A. Hellberg, W.A. Hereman, Phys. Rev. E **86**, 036402 (2012)
26. E.F. El-Shamy, W.F. El-Taibany, E.K. El-Shewy, K.H. El-Shorbagy, Astrophys. Space Sci. **338**, 279 (2012)
27. J.N. Han, Y.L. He, Y. Chen, K.Z. Zhang, B.H. Ma, Phys. Plasmas **20**, 012122 (2013)
28. I. Kourakis, S. Sultana, F. Verheest, Astrophys. Space Sci. **338**, 245 (2012)
29. N.J. Zabusky, M.D. Kruskal, Phys. Rev. Lett. **15**, 240 (1965)